Metabolomics (2013) 9:642–656
DOI 10.1007/s11306-012-0488-3

ORIGINAL ARTICLE

Metabolomic analyses show that electron donor and acceptor ratios control anaerobic electron transfer pathways in *Shewanella oneidensis*

Hui Wang · Elon Correa · Warwick B. Dunn · Catherine L. Winder · Royston Goodacre · Jonathan R. Lloyd

Received: 31 August 2012 / Accepted: 4 December 2012 / Published online: 24 December 2012

Abstract This study investigated the physiological impact of changing electron donor–acceptor ratios on electron transfer pathways in the metabolically flexible subsurface bacterium *Shewanella oneidensis*, using batch and chemostat cultures, with an azo dye (ramazol black B) as the model electron acceptor. Altering the growth rate did result in changes in biomass yield, but not in other key physiological parameters including the total cytochrome content of the cells, the production of extracellular flavin redox shuttles or the potential of the organism to reduce the azo dye. Dramatic increases in the ability to reduce the dye were noted when cells were grown under conditions of electron acceptor (fumarate) limitation, although the yields of extracellular redox mediators (flavins) were similar under conditions of electron donor (lactate) or acceptor limitation. FT-IR spectroscopy confirmed shifts in the metabolic fingerprints of cells grown under these contrasting conditions, while spectrophotometric analyses supported a critical role for *c*-type cytochromes, expressed at maximal concentrations under conditions of electron acceptor limitation. Finally, key intracellular metabolites were quantified in batch experiments at various electron donor and acceptor ratios and analysed using discriminant analysis and a Bayesian network to construct a central metabolic pathway model for cells grown under conditions of electron donor or acceptor limitation. These results have identified key mechanisms involved in controlling electron transfer in *Shewanella* species, and have highlighted strategies to maximise reductive activity for a range of bioprocesses.

Keywords Electron transport · Cytochrome *c* · Flavins · Azo dye · Bayesian networks · Metabolism

1 Introduction

Shewanella oneidensis MR-1, a Gram-negative dissimilatory metal-reducing bacterium, is able to conserve energy

Electronic supplementary material The online version of this article (doi:10.1007/s11306-012-0488-3) contains supplementary material, which is available to authorized users.

H. Wang · J. R. Lloyd (✉)
School of Earth, Atmospheric and Environmental Sciences and Williamson Research Centre of Molecular Environmental Science, University of Manchester, Manchester M13 9PL, UK
e-mail: jon.lloyd@manchester.ac.uk

H. Wang
e-mail: hui.wang@manchester.ac.uk

H. Wang
Faculty of Life Science, University of Manchester, Oxford Road, Manchester M13 9PT, UK

E. Correa · R. Goodacre
School of Chemistry, Manchester Institute of Biotechnology, University of Manchester, 131 Princess Street, Manchester M1 7DN, UK

W. B. Dunn
Institute of Human Development, The University of Manchester, Manchester, UK

W. B. Dunn
Centre for Advanced Discovery and Experimental Therapeutics, Central Manchester University Hospitals NHS Foundation Trust, Manchester Academic Health Sciences Centre, Manchester, UK

C. L. Winder
School of Chemical Engineering and Analytical Science, Manchester Institute of Biotechnology, University of Manchester, 131 Princess Street, Manchester M1 7DN, UK

for growth via the oxidation of carbon substrates including lactate or hydrogen to the reduction of a wide range of electron acceptors such as fumarate, sulfur compounds, fuel cell anodes and various metals including insoluble metal oxides (Myers and Nealson 1990; Myers and Myers 1993; Coates and Achenbach 2002; Wang et al. 2010). There have been rapid advances in the understanding of the complex physiology of *S.oneidensis*, supported by the availability of the complete genome sequence for this organism (Heidelberg et al. 2002) and 23 other *Shewanella* species sequenced to date (see http://www.jgi.doe.gov/genome-projects). Most recent publications have focused on elucidating the proteins and corresponding genes required for the respiration of high oxidation state metals using biochemical and post-genomic techniques (Coursolle and Gralnick 2010; Clarke et al. 2011).

Direct enzymatic and indirect "redox-mediator" driven mechanisms have been proposed for electron transfer to soluble and insoluble electron acceptors in *Shewanella* species (Newman and Kolter 2000). The most intensively studied direct electron transfer mechanism involves the transfer of electrons to extracellular electron acceptors (e.g. Fe(III) or Mn(IV) oxides) via well documented *c*-type cytochromes localised in the outer membrane (Myers and Myers 1993). Cytochromes play an important role in shuttling electrons between different components of the electron transport chain via iron-containing heme cofactors (Myers and Myers 1997b; Myers and Myers 2004), and are up regulated during anaerobic growth (Myers and Myers 1993; Myers and Myers 2000), which have been shown to play a role in electron transfer from the cytoplasmic membrane, through the periplasm to the outer membrane (Myers and Myers 1997a, b; Wang et al. 2010b). Soluble electron acceptors that can traverse the outer membrane, e.g. chelated Fe(III) may also interact directly with periplasmic *c*-type cytochromes negating the requirement for direct interactions with cytochromes exposed on the surface of the outer membrane (Myers and Myers 1993). An alternative indirect mechanism for the reduction of extracellular electron acceptors such as Fe(III) oxides by *Shewanella* species is to utilise soluble "electron shuttles" which can transfer electrons from the surface of the cell to the poorly soluble electron acceptor (Hernandez and Newman 2001). Humic substances (Lovley et al. 1996) and water-soluble quinones (Newman and Kolter 2000) have been shown to act as electron shuttles to stimulate the rapid reduction of insoluble terminal electron acceptors by *S. oneidensis* MR-1. More recently, flavins (Flavin mononucleotide (FMN) and riboflavin) were identified as the endogenous electron shuttles secreted by *Shewanella* species, and shown to accelerate the reduction of Fe(III) oxides, azo dyes (von Canstein et al. 2008) and the anode of a microbial fuel cell (Marsili et al. 2008). Several recent publications have also suggested that Fe(III) reduction can be mediated by extracellular "nanowires" by subsurface Fe(III)-reducing bacteria including *Geobacter* (Reguera et al. 2005) and *Shewanella* species (Gorby et al. 2006), offering an alternative pathway for long-range indirect reductions.

Although there is much interest in the physiology of metal-reducing bacteria, recent advances in "metabolomics" research (Brown et al. 2005; Goodacre et al. 2007) have not been applied to these bioprocesses. The first step needed to identify the actual changes observed in the intracellular central metabolism (Cornish-Bowden and Luz Cardenas 2000) is to quantify the concentrations of primary intracellular metabolites and map these onto central metabolic pathways (for example, TCA cycle). Several steps need to be considered in this process (Goodacre et al. 2004). The first is that metabolism turns over very quickly and thus effective quenching is needed as described for the closely related *Escherichia coli* (Winder et al. 2008), following this the metabolites are extracted from the cellular biomass; the samples are then ready for analysis. As metabolites in central metabolic pathways (for example, TCA cycle) are being targeted, gas chromatography–mass spectrometry is preferred for metabolomics studies (Sumner et al. 2007; Winder et al. 2011), following strict protocols for sample preparation (Sumner et al. 2007; Dunn et al. 2011a) and a range of data processing are used within the metabolomics pipeline (Brown et al. 2005) to assure that any inferences from the data are valid, and these should follow accepted standards (Goodacre et al. 2007).

In this study, a chemostat was used to investigate the metabolic state of *S. oneidensis* MR-1 grown anaerobically at a range of dilution (growth) rates under conditions of electron acceptor limitation, prior to investigating the impact of varying the ratio of electron donor to electron acceptor, encompassing conditions of electron donor excess and limitation. In all experiments, lactate was used as the electron donor and fumarate as the electron acceptor and various components of direct and indirect extracellular electron transfer mechanisms were quantified. First, the cytochrome-*c* content of the cultures was measured spectrophotometrically after reaction with pyridine nucleotide. Secreted flavin electron shuttles were also quantified by HPLC (high performance liquid chromatography), and the presences of extracellular "nanowires" hypothesised to play a role in extracellular electron transfer (Gorby et al. 2006) were also investigated using environmental scanning electron microscopy (ESEM). The metabolic fingerprints of cultures grown with different electron donor and acceptor ratios were also recorded by FT-IR spectroscopy and compared using multivariate analyses (Wang et al. 2010a). The ability to reduce a model industrially relevant electron acceptor was also quantified using the azo dye

remazol black B (Pearce et al. 2006). Finally, an intracellular metabolic network was constructed in four steps: (i) *S. oneidensis* MR-1 cells were grown in minimal medium in batch cultures with defined concentrations of electron donor (lactate) and acceptor (fumarate), (ii) the key intracellular metabolites were quantified by GC–MS, (iii) the relationships among metabolites and correlations to cell phenotype were analysed by principal components analysis (PCA) and a Bayesian network (BN), (iv) construction and semi-quantification of the central metabolic pathways based on the PCA and BN.

2 Materials and methods

2.1 Bacterial strains and growth medium

Shewanella oneidensis strain MR-1 was obtained from the Manchester University Geomicrobiology group culture collection and stored at −80 °C in 50 % glycerol prior to use. All cultures used were grown in the fully defined minimal medium, based on the recipe of Myers (Myers and Myers 1992). An amino acid solution (20 mg L^{-1} L-arginine hydrochloride, 20 mg L^{-1} L-glutamate, 20 mg L^{-1} L-serine) was also added. Sodium DL-lactate was used as the carbon source and electron donor while fumarate was used as the electron acceptor. The medium was sparged with nitrogen and the pH was adjusted to 7.6 before sterilization. All chemicals were purchased from Sigma unless noted otherwise.

2.2 Continuous and batch cultures

Steady-state continuous cultures were established using a 6 L autoclavable bioreactor (Applikon Biotechnology) containing the defined medium described above with different concentrations of lactate and fumarate. Agitation was maintained at 150 rpm, and pH was monitored continuously. N_2 was delivered at a rate of 0.8 L min^{-1}, and dissolved O_2 tension was monitored using a polarographic O_2 probe. An electrical temp jacket on the fermentor is used to keep the temperature of the stirred chemostat culture constant at 30 °C.

The inoculum for the 3 L fermentor was prepared by injecting 60 mL stationary phase culture grown anaerobically in the same defined medium for ~12 h. The organism was grown to early log phase, and then the chemostat mode was switched on and the operating liquid volume was maintained at 3 L at a range of flow (dilution) rates. For the medium containing 100 mM lactate and 20 mM fumarate, flow rates of 0.07, 0.18 and 0.25 L h^{-1} were used, equivalent to 10, 40, and 70 % of the maximum growth rate respectively (the maximum growth rate was determined in batch culture as 0.14 h^{-1}); For the medium containing 50 mM lactate and 50 mM fumarate, the maximum growth rate was determined in batch culture as 0.07 h^{-1}, the flow rate was set at 0.15 L h^{-1}, corresponding to 70 % of the maximum growth rate. For the medium containing 20 mM lactate and 100 mM fumarate, the maximum growth rate was determined in batch culture as 0.03 h^{-1} and the flow rate was set at 0.07 L h^{-1}, equivalent to 70 % of the maximum growth rate.

To provide adequate replication for the quantification of intracellular metabolites, batch cultures were prepared in 100 mL serum bottles for GC–MS analysis. Anaerobic cultures were grown in 80 mL of defined minimal medium (flushed with N_2 for 10 min and sealed with a butyl rubber stopper before use, Bello Glass, Inc.). Inocula for these experiments were grown overnight anaerobically at 30 °C to early exponential phase. A 10 mL aliquot of the "starter" culture was used to inoculate six biological replicates "experimental" cultures, which were incubated without agitation at 30 °C. Samples were withdrawn regularly for OD analysis at 600 nm.

2.3 Quantification of cytochromes *c*

The heme content of cell samples was determined by means of pyridine hemochrome analyses. Cytochrome quantification was carried out by measuring the difference between the absorption in the reduced and oxidized states. A molar extinction coefficient of 21.84 mM^{-1} cm^{-1} (oxidation minus reduction absorption at 550 nm) for heme *c* was used for the calculation (Berry and Trumpower 1987). Cytochrome values were normalized by protein concentrations to compare with those of other cells grown in different media.

2.4 Quantification of flavins by HPLC

Cultures for analyses of extracellular flavins were grown in minimal medium as described above. Reverse-phase high performance liquid chromatography (HPLC) was used to separate and quantify the flavins. A Gemini 5 μ C18 110A column (250 × 10.0 mm dimensions; Phenomenex, UK) was used, fitted to a GP50 gradient pump and UVD170U UV–vis detector, both from Dionex, UK. Samples (1 mL) were harvested by centrifuge at 13,000 *g* for 20 min and the supernatants analyzed for extracellular flavins. The programmes of HPLC for flavins quantification have been previously described (von Canstein et al. 2008; Wang et al. 2010a). Peak areas were calculated using Chromeleon software (version 6.50, Dionex). The concentrations of unknown samples were calculated by comparison with a graph prepared from the standards.

2.5 Environmental scanning electron microscopy (ESEM)

Samples for ESEM were removed from chemostat cultures and fixed immediately using an anaerobic solution of glutaraldehyde (2 % v/v final concentration). Samples were carefully applied to membrane filters with a 0.2 μm pore size and washed gently with pH 7.4 phosphate buffered saline (PBS, NaCl, 8.0 g L^{-1}; KCl, 0.2 g L^{-1}; $Na_2HPO_4{\cdot}2H_2O$, 1.44 g L^{-1}; KH_2PO_4, 0.24 g L^{-1}), dilute PBS (50:50 with deionized water), and then deionized water. A Polaron SC7640 High Resolution Sputter Coater was used to coat the gold onto the surface of the sample. The samples were imaged using a Philips XL30 FEG Environmental Scanning Electron Microscope (FEI, Netherlands). The ESEM was used to scan the surface area with accelerating voltages of 10 and 20 kV at both low and high magnifications using the secondary electron detector to image the sample (SEI).

2.6 Azo dye reduction

To determine the potential of cells of *S. oneidensis* MR-1 grown under a range of growth regimes to reduce an added electron acceptor, the azo dye Remazol Black B was added to washed cell suspensions (Pearce et al. 2006) and dye reduction monitored spectrophotometrically at 597 nm, using a Specord S100 spectrophotometer. An Analytik Jena AG SPECORD 600 UV/vis eightfold cell changer was fitted to the spectrophotometer and a water bath (Grant Instruments Ltd GD120, Cambridge) was used to maintain the temperature of the samples at 30 °C. The A_{597} was measured in sealed anaerobic vials, under a headspace of N_2, to maintain anaerobic conditions. Solutions of Remazol Black B reactive dye were added to the auto-sampler vials (size 5 mL) to a final concentration of 25 μM. Sodium lactate was added to the vials as the electron donor (final concentration, 10 mM). Riboflavin (10 μM) was added where indicated as an electron shuttle. The mixture was buffered with phosphate buffered saline (NaCl, 8.0 g L^{-1}; KCl, 0.2 g L^{-1}; $Na_2HPO_4{\cdot}2H_2O$, 1.44 g L^{-1}; KH_2PO_4, 0.24 g L^{-1}, pH 7.4) to a finally volume of 4 mL. An anaerobic suspension of washed cells (0.5 mL) was injected, by use of a syringe that was fitted with a hypodermic needle, into the sealed anaerobic vials.

Absorbance measurements started immediately after the cells were injected into the vials. Absorption of the solution was measured at a spectrum from 200 to 700 nm periodically by WinASPECT software (version 2.0.4.112). The absorbance of 'blank' solutions, containing everything but the dye, were also measured and used to normalise the absorbance data that were obtained from the solutions containing the dye.

2.7 Fourier transform infrared spectroscopy analysis

The metabolic fingerprints of cells grown aerobically and anaerobically were recorded by FT-IR periodically. All FT-IR spectroscopy analysis was conducted using an Equinox 55 infrared spectrometer equipped with a high throughput motorised microplate module, HTS-XT^{TM} (Bruker Optics, Coventry, UK). Samples (5 mL) were collected and centrifuged at 4 °C at 12,000×*g* for 10 min, the supernatant was removed and the cell pellet was washed twice with sterile 0.9 % NaCl solution and centrifuged again prior to storage at −80 °C. FT-IR analyses for all the samples have been previously described (Wang et al. 2010a). The ASCII data were imported into Matlab version 6 (The MathWorks) and extended multiplicative scatter correction (EMSC) (Martens and Stark 1991), and row normalisation pre-processing steps were applied prior to PCA.

2.8 GC–MS

Gas chromatography-mass spectrometry (GC–MS) was used to analyse intracellular metabolites in a range of cultures. To quench the metabolism of the cells, the cultures were rapidly sprayed into quenching solution (60 % aqueous methanol solution, pre-cooled to −48 °C) at 3:1 ratio of quenching solution to culture. The biomass was harvested at −4 °C at 13,000 *g* for 10 min and the supernatant was removed prior to storage at −80 °C. Extraction of the intracellular metabolites was performed on the lyophilised biomass. The protocol to derivatise the metabolites for GC–MS analysis has been previously described (Begley et al. 2009; Dunn et al. 2011b). Here, lyophilised extracts were chemically derivatised in a two-step process. Step 1 involved addition of 50 μL of a 20 mg ml^{-1} *O*-methoxylamine in pyridine solution to the dried extract, followed by thorough mixing for 15 s on a vortex mixer, and then heating in the Dri-Block heater at 80 °C for 15 min. Step 2 involved addition of 50 μL of *N*-methyl-*N*-trimethylsilyltrifluoroacetamide, vortex mixing for 15 s and heating in a block heater at 80 °C for 15 min. 20 μL of a retention index solution (0.6 mg mL^{-1} of C_{10}, C_{12}, C_{15}, C_{19} and C_{22} *n*-alkanes dissolved in pyridine) was added followed by centrifugation and transfer of 90 μL of the solution to a 2 mL vial containing a 300 μL insert and sealed with a septum containing screw cap. Samples were analysed on a Leco Pegasus III electron-impact mass spectrometer (Leco Corp., St. Joseph, MO) coupled to a model 6890 N gas chromatograph with a split/splitless injector (Agilent Technologies, Stockport, UK), according to the method for yeast metabolite footprints described in (O'Hagan et al. 2004). Data were pre-processed as described in previous report (MacKenzie et al. 2008)

to provide a data matrix (sample vs. metabolic feature and inputted with chromatographic peaks areas if metabolic feature was detected in sample) for further data analysis. Metabolic features were assigned metabolite identifications by comparison of the retention index and mass spectrum for sample to those present in an in-house mass spectral library (Manchester Metabolomics Database, MMD) constructed using authentic chemical standards analysed under identical analytical conditions (Brown et al. 2009). A definitive identification (Metabolomics Standards Initiative chemical analysis class (Sumner et al. 2007)) was assigned if the match was greater than 70 % and the retention index of sample and library matched ± 10. A putative annotation (Metabolomics Standards Initiative chemical analysis class 2 or 3 (Sumner et al. 2007)) was assigned if the mass spectral match was greater than 70 % in comparison to two mass spectral libraries (Golm Metabolome Database (Kopka et al. 2005) and NIST05). The process of chemical derivatization can produce two or more chemical derivatives and therefore a single metabolite can be detected as multiple metabolic features. All the GC–MS data was normalized by biomass concentration to eliminate the reflections of the biomass variation.

2.9 Principal components analysis (PCA)

The objective of PCA is to explain the variance–covariance structure of a set of variables through a few linear combinations of these variables (Johnson and Wichern 2007). Much of the original data variability can be accounted for by a small number of principal components which are then used for data reduction and visual data interpretation. The PCA results are discussed in terms of component scores and loadings. The component scores are the transformed variable values and the loadings are the weights by which the original data variables should be multiplied to obtain the component scores. A combination of component scores and loadings, also known as biplot, is frequently used to visualise correlations between groups of samples and variables, cell type and metabolites respectively in this study. Before applying PCA data have been autoscaled so that each data column, corresponding to a variable (metabolite), has a mean equal to zero and a standard deviation equal to 1. In addition, to remove noise from the FT-IR spectra and reduce differences caused only by shift on spectral intensity. We apply extended multiplicative scatter correction (EMSC) on all spectra before analysis. The EMSC method has originally been developed to reduce the disturbing effect of light-scattering, small particles scatter light more than larger ones. This type of normalization takes the information registered in the spectra and attempts to separate physical light-scattering effects from the actual light absorbed by molecules (Martens and Stark 1991). We used the R v. 2.9.2 software (R: A Language and Environment for Statistical Computing, Vienna, Austria, 2012, http://www.R-project.org) to perform the PCA computations. Figure 2b shows the biplot computed for the cell types and metabolites from *S. oneidensis* MR-1.

2.10 Bayesian network analysis

A Bayesian network (BN) is a graphical map of the probabilistic relationships among variables of a given problem domain (Pearl 1988). In this work the variables are the metabolites assayed via GC–MS. The BN was implemented according to (Correa and Goodacre 2011). The graphical model of a BN is represented by nodes and arrows. The nodes represent variables from the problem (e.g., metabolites) and an arrow linking two nodes indicates a statistical correlation between them. Contrary to intuition, the direction of the arrow on a BN does not necessarily imply a cause-effect relationship between variables. A BN model is not a "causal network". A causal network is a BN with an explicit requirement that the relationships (arrow directions) be causal (Pearl 2000). Causal networks are out of the scope of this paper and are a subject for future work.

Therefore, to eliminate the possible misleading cause-effect interpretation from our BN model, we intentionally omit the arrow heads from the graph. On the BN generated from our data a line linking two metabolites implies that there is a statistically significant relationship between them; detected during the network building process. After learning the network structure (Correa and Goodacre 2011), we also compute the Pearson's correlation coefficient (and its respective p value) between linked metabolites and show these number on the network. The data matrix used to build the BN models is as follows. Rows of the matrix represent measured samples of *S. oneidensis*. There are 8 replicates for each of treatments applied, namely, L70F50, L60F60, L50F70 and L40F80. Columns represent the specific metabolites measured by GC–MS. Data have been autoscaled before building the BN models. Each of the 14 metabolites (variables) analyzed is individually represented by a node on the graph of the BN. To evaluate the score of the candidate networks we used the Bayesian Dirichlet method described in (Cooper and Herskovits 1992). The scripts for the BN analysis were developed in-house using MATLAB v. 2009a (The MathWorks Inc., Natick, Massachusetts, USA.) and are available from the authors on request. The results of the BN analysis applied to the 32 samples by 14 metabolites data matrix are shown in Fig. 3.

3 Results

3.1 Impact of dilution rates, electron donor and acceptor ratios on electron transfer mechanisms and azo dye reduction

3.1.1 Growth yield of S. oneidensis *MR-1 in minimal medium*

To determine the impact of varying the dilution and hence growth rate on key physiological parameters of anaerobically grown cells of *S. oneidensis* MR-1, the organism was cultivated in a chemostat using defined minimal medium containing 100 mM lactate and 20 mM fumarate at 3 different dilution rates. These were 0.42, 0.28 and 0.07 L h^{-1} corresponding to 70, 40 and 10 % of the maximum specific growth rate (μmax) measured in 3 L batch cultures in a fermenter. Initial measurements focused on the growth yields at various dilution rates, quantified by measuring total protein and conversion to dry weight biomass assuming by comparison to appropriate standard curves prepared using freshly grown cells (Table 1). The growth yield of *S. oneidensis* MR-1 was highest at 70 % of μmax, with an average of 35 mg L^{-1} dry weight biomass. When grown at 10 and 40 % of μmax, biomass yields were lower, with an average of 25 and 29 mg L^{-1} respectively.

Continuous growth in a chemostat was obtained at various ratios of electron donor to electron acceptor by manipulating the different concentrations of fumarate and lactate in a fully defined minimal medium. The specific growth rate was fixed at 70 % of μmax measured at three different electron acceptor and donor ratios (100 mM lactate: 20 mM fumarate, 50 mM lactate: 50 mM fumarate or 20 mM lactate: 100 mM fumarate). This translated to a dilution/growth rate for *S. oneidensis* MR-1 between 0.03 and 0.14 h^{-1} for the different electron donor: acceptor ratios. For the minimal medium containing 100 mM lactate and 20 mM fumarate, the lactate was in excess and the fumarate was the growth-limiting substrate. For the minimal medium containing 20 mM lactate and 100 mM fumarate, the fumarate was in excess and the lactate was the growth-limiting substrate. This was confirmed by HPLC analysis of the organic acids in the medium (data not shown). In the 50 mM lactate/50 mM fumarate medium, fumarate was the limiting substrate according to HPLC analysis.

The ratio of lactate to fumarate in the medium resulted in an obvious impact on the biomass yields (Table 1). For the medium containing 50 mM lactate and 50 mM fumarate, the biomass concentration was 85 mg L^{-1} dry weight, while with the ratio of lactate to fumarate of 20–100 mM, the biomass concentration decreased slightly to 68 mg L^{-1}. With the lactate supplied at 100 mM and the fumarate at 20 mM, the biomass yield was the lowest, reaching only about 38 mg L^{-1}.

3.1.2 Cytochrome c *content*

The impact of varying the dilution rate on the cytochrome *c* content of the cells was also quantified by spectrophotometric analysis after reaction with pyridine. These analyses showed that the cytochrome content was similar irrespective of the dilution rate imposed. At all dilution rates, the cytochrome yield was ~8 μmol g^{-1} protein (Table 1).

The cytochrome *c* content of the cells grown in the medium containing 50 mM lactate and 50 mM fumarate were quite similar to that of the cells grown in the 100 mM lactate and 20 mM fumarate medium (about 9.1 and 8.7 μmol g^{-1} protein respectively, presented in Table 1). The cytochrome *c* content of the cells grown in the 20 mM lactate and 100 mM fumarate medium was much lower, about 0.8 μmol g^{-1} protein, equating to 10 % of that of the *S. oneidensis* MR-1 cells grown in the minimal medium with other two lactate:fumarate ratios. Also, there was a distinct difference in the colours of the three cultures. Cells grown in medium limited by electron acceptor (100 mM lactate and 20 mM fumarate) were a bright pink colour

Table 1 Physiology parameters of *S. oneidensis* MR-1 in minimal medium with three different electron donor and acceptor ratios

Samples	DR (%)	Biomass (mg L^{-1})	Cytochrome *c* (μmol g $protein^{-1}$)	FMN	
				(μM)	(μmol mg $protein^{-1}$)
L100F20	10	24.6 (3.30)	7.8 (0.87)	0.08 (0.002)	1.8 (0.04)
	40	28.9 (4.94)	8.7 (0.04)	0.13 (0.006)	2.2 (0.10)
	70	35.3 (10.03)	8.7 (0.01)	0.13 (0.001)	2.3 (0.01)
L50F50	70	85.2 (6.39)	9.1 (0.11)	0.25 (0.042)	5.4 (0.62)
L20F100	70	68.1 (10.44)	0.8 (0.78)	0.22 (0.040)	3.3 (0.99)

Numbers in brackets indicate standard deviations of measurements from 5 biological replicates

L100F20 medium containing 100 mM lactate, 20 mM fumarate; *L50F50* medium containing 50 mM lactate, 50 mM fumarate; *L20F100* medium containing 20 mM lactate, 100 mM fumarate; *DR* stands for the dilution rates of the max growth rates

indicative of a high cytochrome *c* content, whereas cells grown with an excess of fumarate (20 mM lactate and 100 mM fumarate) had a creamy-white colour consistent with a much lower cytochrome content. Cells grown at the intermediate lactate: fumarate ratios were beige in colour.

3.1.3 Secretion of flavins

The concentrations of flavin compounds secreted by *S. oneidensis* MR-1 and shown to act as extracellular redox shuttles (von Canstein et al. 2008) were quantified using HPLC (Table 1). The predominant flavin secreted by all continuous cultures of the organism in the 100 mM lactate and 20 mM fumarate minimal medium was FMN, with only trace amount of riboflavin detected. The intracellular flavin FAD could not be detected at any dilution rate, suggesting that cell lysis which would release this flavin was minimal. The extracellular concentration of FMN was highest (0.13 μM) when the organism was grown at 70 and 40 % of μmax, with only 0.08 μM measured when the cells were grown at 10 % of μmax. When the yields of FMN were normalised to biomass levels, similar trends across the dilutions rates were noted (70 = 40 % >10 % of μmax).

The ratio of lactate to fumarate in the medium seemed to have a discernible impact on the specific yield of FMN normalized to biomass levels. The results are summarized in Table 1. The yield of FMN was highest when cells were grown in minimal medium with lactate and fumarate both supplied at 50 mM (5.36 μmol FMN mg protein^{-1}), while in 20 mM lactate:100 mM fumarate medium and 100 mM lactate:20 mM fumarate medium the yields were 3.27 and 2.33 μmol FMN mg protein^{-1} respectively.

3.1.4 Azo dye bioreduction

To quantify the impact of dilution rate and altering the electron donor:acceptor ratio on electron transfer processes, azo dye reduction and decolouration was quantified by assaying the dye reduction activity of *S. oneidensis* MR-1 cell suspensions, harvested from the chemostat containing minimal medium. The influence of riboflavin as an electron shuttle on the rate and extent of dye reduction was also examined. All these results are summarized in Table 2. The rates of reduction noted were very similar irrespective of the dilution rate used in the absence of added riboflavin (Table 2). Specific rates of reduction were 577, 522, and 508 μmol dye min^{-1} g protein^{-1} for the cultures grown at 10, 40 and 70 % of μmax respectively. However, when 10 μM riboflavin was added, the specific rates of reduction were far higher in the cultures grown at 10 % of μmax (1,099 μmol dye min^{-1} g protein^{-1}, versus 762 μmol dye min^{-1} g protein^{-1} and 663 μmol dye min^{-1} g protein^{-1}for the cultures grown at 40 and 70 % of μmax). In these experiments, all cultures were able to completely decolourise the azo dye via bioreduction in 1 h.

The dye reduction rates were highest with cells grown in electron acceptor-limited medium (100 mM lactate and 20 mM fumarate minimal medium) with a specific rate of dye reduction of 508 μmol dye min^{-1} g protein^{-1} recorded. For the cells grown in electron acceptor excess medium (the 20 mM lactate and 100 mM fumarate), the specific rate of dye reduction dropped dramatically to 5 μmol dye min^{-1} g protein^{-1}, and in the 50 mM lactate and 50 mM fumarate minimal medium a similar very low value was recorded. With the addition of riboflavin as an extracellular electron shuttle, the specific rates of dye reduction increased in each of the three chemostat cultures, reaching 663 μmol dye min^{-1} g protein^{-1} with cells from electron acceptor limited medium (the 100 mM lactate and 20 mM fumarate minimal medium), 430 μmol dye min^{-1} g protein^{-1}with cells from the 50 mM lactate and 50 mM fumarate minimal medium, and 23 μmol dye min^{-1} g protein^{-1} when the 20 mM lactate and 100 mM fumarate minimal medium (electron donor limited) was used.

3.2 FT-IR analysis of the fingerprints of *S. oneidensis* MR-1 cells

To compare the metabolic fingerprints of *S. oneidensis* MR-1 cells grown in the chemostat at a range of dilution rates, infrared absorption spectra were collected from cells cultured in medium containing 100 mM lactate and 20 mM fumarate and analysed by PCA (Supplementary Fig. S1). FT-IR analysis indicated clearly that the dilution rate had little impact on the metabolic fingerprints of the cells (Supplementary Fig. S1). However, when cells were grown in the chemostat with three electron donor: acceptor ratios, hierarchical cluster analysis (Fig. 1) showed a clear effect when the cells were grown under conditions of electron donor limitation (in 20 mM lactate:100 mM fumarate minimal medium), suggesting that the physiology and metabolism of the cells had changed dramatically under these conditions.

The corresponding key bands contributing to these separations were identified by examining of loading plots (Supplementary Table S1). The separation between cells grown on electron donor limited medium and electron acceptor limited medium was characterised mainly by the 1182–1037 and 1635–1610, 1535–1512 cm^{-1} regions, which represented contributions from the phosphate, carbohydrate absorption vibrations and amide I and II protein related vibrations respectively (Wang et al. 2010a). In addition, the 2,960–2,900 and 2,860–2,844 cm^{-1} region,

Table 2 Impact of e-donor to e-acceptor ratio on azo-dye reduction

Samples	DR (%)	Dye reduction rates (μM dye min^{-1})	Specific dye reduction rates (μmol dye (min g protein)$^{-1}$)	Dye reduction rates with RF (μM dye min^{-1})	Specific dye reduction rates with RF (μmol dye (min g protein)$^{-1}$)
L100F20	10	27.3 (16.08)	577.25	51.29 (16.08)	1099.30
	40	29.7 (10.22)	521.97	43.30 (1.01)	761.84
	70	28.9 (0.30)	507.54	43.11 (7.24)	663.11
L50F50	70	0.4 (0.1)	4.76	36.12 (3.04)	429.85
L20F100	70	0.3 (0.08)	4.75	1.42 (0.21)	23.33

Legend same as Table 1. Numbers in brackets indicate standard deviations of measurements from 5 biological replicates

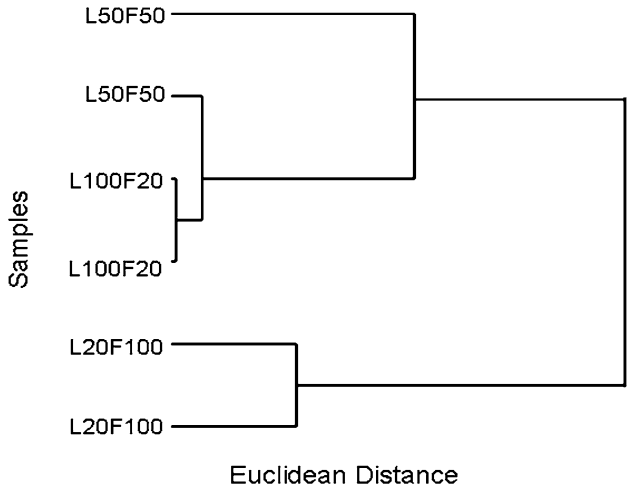

Fig. 1 HCA dendrogram constructed on the IR data showing effect of different ratios of e^--donor and e^--acceptor

which corresponded to phospholipids and lipids (Wang et al. 2010a) was also highlighted as being discriminatory for cells grown in medium with equal concentrations of electron donor: acceptor (50 mM lactate:50 mM fumarate) (Supplementary Table S1).

3.3 Environmental scanning electron microscopy of *S. oneidensis* MR-1 cells grown with various electron donor and acceptor ratios

It has been reported that *S. oneidensis* MR-1 can produce electrically conductive proteinaceous nanowires in response to growth under conditions of electron acceptor limitation (Reguera et al. 2005; Gorby et al. 2006). However, ESEM analysis of the chemostat cultures of *S. oneidensis* MR-1 grown at the three electron donor–acceptor ratios used in our study, including cells grown under conditions of electron acceptor limitation (100 mM lactate and 20 mM fumarate minimal medium), showed no evidence for these extracellular appendages under any of the conditions imposed in our experiments (Supplementary Fig. S2).

3.4 Impact of electron donor and acceptor ratios on cellular metabolism

3.4.1 Cytochrome c content analysis

To explore the physiological impact of varying the electron donor and acceptor ratios during growth further, *S. oneidensis* MR-1 was grown in batch cultures in minimal medium containing lactate to fumarate ratios varied between 20 mM lactate: 100 mM fumarate (electron donor limited) and 100 mM lactate:20 mM fumarate (electron acceptor limited) respectively. The aim of this experiment was to find the tipping point, where changes in electron donor: acceptor ratio impact on cytochrome content, and hence electron transfer processes such as dye and metal reduction. These experiments were a precursor to GC–MS analyses of the intracellular metabolome of *S. oneidensis*. The profiles of growth, lactate and fumarate consumption of seven medium compositions between these ratios are shown in Supplementary Table S2. The fumarate concentrations remaining in cultures with 70 mM lactate and 50 mM fumarate (or electron donor: acceptor ratios in excess of this) were below the limit of detection ($\sim$10 μM) confirming electron acceptor limitation. When ratios of lactate to fumarate were reduced, concentrations of the lactate remaining in the cultures decreased, and the cultures became electron donor limited. In these experiments, the cellular cytochrome *c* concentrations showed a significant increase when lactate: fumarate ratios increased above 60 mM lactate: 60 mM fumarate, and the cultures moved towards conditions of electron acceptor (fumarate) limitation (Fig. 2a). On the basis of the data presented in Fig. 2a, four ratios of lactate to fumarate were selected for the GC–MS study (70 mM lactate:50 mM fumarate, 60 mM lactate: 60 mM fumarate, 50 mM lactate:70 mM fumarate and 40 mM lactate:80 mM fumarate), around the tipping point for increased cytochrome expression, which was between 60 mM lactate: 60 mM fumarate, 50 mM lactate:70 mM fumarate in the defined medium used.

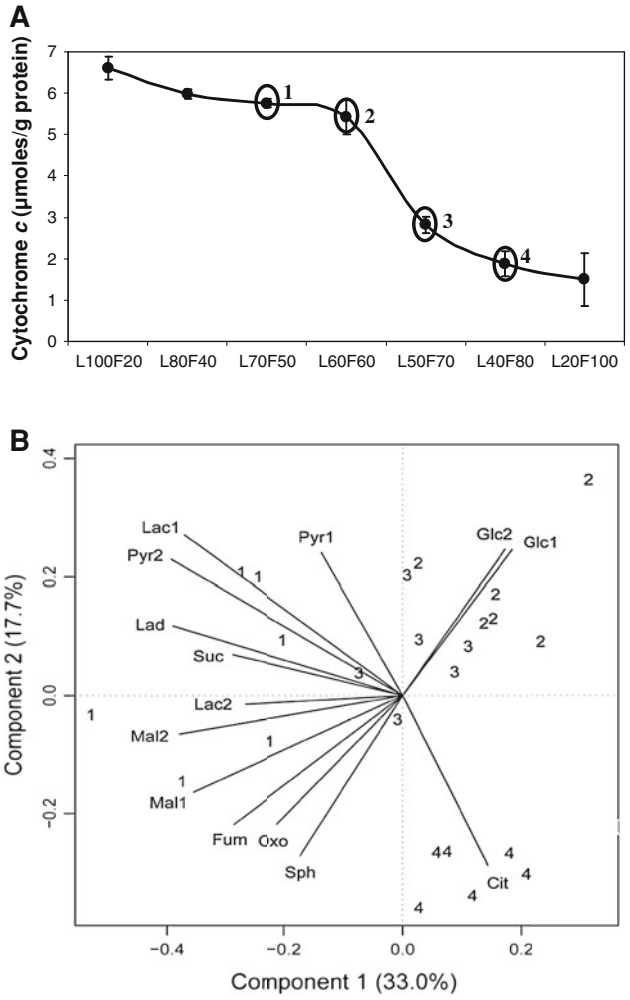

Fig. 2 The effects of lactate and fumarate feeding ratios on cellular cytochrome *c* (**a**) and PCA biplot for the metabolites from *S. oneidensis* MR-1 cells (**b**). In (**a**) each point shows the biological repeats from 3 measurements, and the *error bars* indicate standard deviations. *1* cells grown in L70F50 medium, *2* cells grown in L60F60 medium, *3* cells grown in L50F70 medium, *4* cells grown in L40F80 medium. See the legend to Fig. 4 for abbreviations. In (**b**) the numbers refer to the location of the samples in the PCA scores plots, whilst the metabolite codes (see the legend to Fig. 4 for abbreviations) represent the loadings vectors for the metabolites

3.4.2 Intracellular metabolites qualification by GC–MS

In order to investigate further the metabolic impact of varying the electron donor: acceptor ratios in anaerobic cultures of *S. oneidensis* MR-1, GC–MS was used to analyze and quantify the intracellular metabolites of *S. oneidensis* MR-1 grown in medium with different lactate: fumarate ratios. The relative concentrations of the metabolites of interest were calculated using appropriate internal standards to facilitate further data analysis. 82 unique chromatographic peaks were detected in the dataset. 22 peaks were definitively identified by matching electron impact mass spectrum and retention index to data of authentic chemical standards present in the Manchester Metabolomics Database (Supplementary Table S3). 15 peaks were putatively annotated based on matching of the electron impact mass spectrum to those of authentic chemical standards in other mass spectral libraries (Golm Metabolome Database (Kopka et al. 2005) and NIST05). These annotated and identified metabolites are defined in Supplementary Table S3. As a result of the chemical derivatization method applied a single metabolite can be produce multiple derivatization products, typically containing different numbers of trimethylsilyl (TMS) groups or attachment of a single TMS group to different functional groups of the same metabolite (for example amine or carboxylic acid groups of amino acids). For example, glucose typically produces two derivatization products. For reference Pyr1 and Pyr2 (as well as for the others similar cases) exist as there were two derivatisation products for these metabolites detected and quantified by GC–MS; we have chosen not to amalgamate the responses for these metabolites.

Initially PCA was used to detect groups of metabolites that strongly correlate with each other and observe their relationships with respect to the different culture conditions. Figure 2b shows the PCA scores and loadings plot for the metabolites from *S. oneidensis* MR-1 cells. The cells are labelled according to their lactate and fumarate concentrations as: 1 = 70 mM lactate:40 mM fumarate, 2 = 60 mM lactate:60 mM fumarate, 3 = 50 mM lactate:70 mM fumarate and 4 = 40 mM lactate:80 mM fumarate. The PC scores plot shows good discrimination between the four different growth conditions, particularly 70 mM lactate: 40 mM fumarate and 40 mM lactate:80 mM fumarate. The graph also shows that citric acid (Cit) is highly correlated with 4 = 40 mM lactate:80 mM fumarate medium, and glucose (Glc1 and Glc2) is highly correlated with 2 = 60 mM lactate:60 mM fumarate. The PC scores and loadings plot also indicate a strong correlation between some metabolites such as lactic acid (Lac1) and pyruvic acid (Pyr2). However, PCA does not give any indication of the strength of these correlations. Therefore, we used a BN model to identify subgroups of metabolites that are correlated and to estimate the strength of these correlations relative to one another.

Figure 3 shows the BN network model built using the same metabolites shown on the PCA plot discussed above. The lines linking metabolites represent statistical correlations. The BN adds to the information provided by PCA. It shows, for instance, that lactic acid (Lac1) and pyruvic acid (Pyr2) have a positive correlation coefficient value equal to 0.79 and the *p* value associated with this correlation less than 0.01; so these are statistically significant. Most strikingly the BN also indicates that there are 2 main subgroups of correlated metabolites. The first subgroup is composed

by pyruvic acid (Pyr2 and Pyr1), lactic acid (Lac1), citric acid (Cit), lactic acid dimer (Lad), succinic acid (Suc) and malic acid (Mal2) and the second one is composed by fumarate (Fum), malic acid (Mal1), sugar phosphate (Sph) and oxoglutaric acid (Oxo).

3.4.3 Intracellular metabolic pathway network model

Biochemical pathways for the central carbon metabolism of *S. oneidensis* MR-1 were generated based on BN results while referring to data from previously published work (Alm et al. 2005; Serres and Riley 2006; Tang et al. 2007a, b). The central metabolic network developed includes the tricarboxylic acid (TCA) cycle, glycolysis, pentose phosphate (Beliaev et al. 2005) pathway, formate-serine pathway, and the fumarate-putrescine pathway. The directions of the reactions were not studied in this research, so are generally marked as reversible in Fig. 4. The relative concentrations of the main intracellular metabolites detected are shown by a colour bar (Fig. 4), and standard deviation of these concentrations were shown in Supplementary Fig. S3.

Lactate, the electron donor supplied, is converted to pyruvate (PYR) by *S. oneidensis* MR-1 and then channelled into three potential routes: the TCA cycle, to formate then the serine-isocitrate lyase pathway, or to phosphoenolpyruvate (PEP) by glycolysis. However, both lactate, and the conversion product pyruvate, were shown to accumulate in cells grown in medium when the electron donor was added to excess (compared to the electron acceptor fumarate) in the order 70 mM lactate:40 mM fumarate >60 mM lactate:60 mM fumarate >50 mM lactate:70 mM fumarate (Fig. 4). Pyruvate was further metabolised to hexose sugars via PEP under conditions of fumarate excess. The intracellular glycolysis and PP pathways (running from pyruvate (PYR) to phosphoenolpyruvic acid (PEP) to glycerol-3-phosphate (PGA) to ribose-5-phosphate (R5P)) noted, may in turn have promoted the increase in biomass recorded under these conditions.

Fumarate was respired to succinate by *S. oneidensis* MR-1 under anaerobic conditions, via fumarate reductase (Taylor et al. 1999), but surprisingly accumulated within the cells, even when fumarate was limiting (Fig. 4). Succinate however was at maximal concentrations when lactate (electron donor) was in excess and fumarate was limiting. Putrescine (PUT) was also detected within the cells when fumarate was supplied in excess. This indicated that fumarate was transformed to arginine (ARG) then

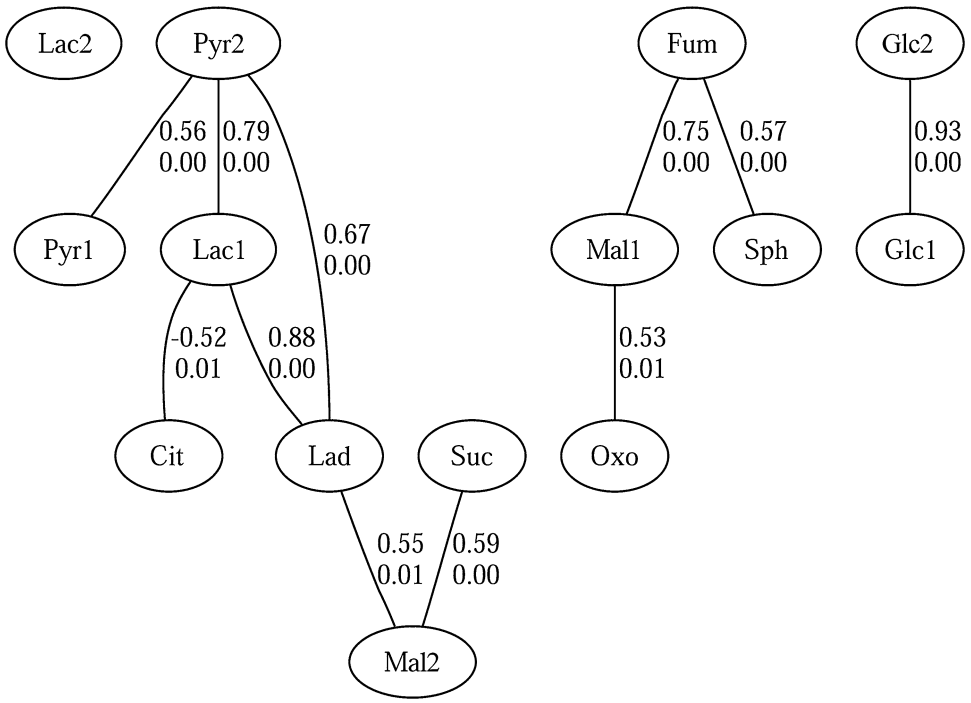

Fig. 3 Bayesian network analysis of the intracellular metabolism of *S. oneidensis* MR-1 cell grown in minimal medium with three different electron donor and acceptor ratios. The numbers shown on the network represent Pearson's correlation coefficient and *p* value respectively; the *p* value allows statistical significance, computed for that correlation to be assessed (all those above were significant and not correlated by chance). See the legend to Fig. 4 for abbreviations.

Note: the reason why Lac2 is not linked to any other metabolite in the network may be because Lac2 is a derivatisation product of lactic acid detected by GC–MS and is present in a very low intensity (see Fig. 4). Likewise, Pyr1, Mal2 are also derivatisation products and are present in low concentrations. Therefore, these metabolites may not show the expected correlations

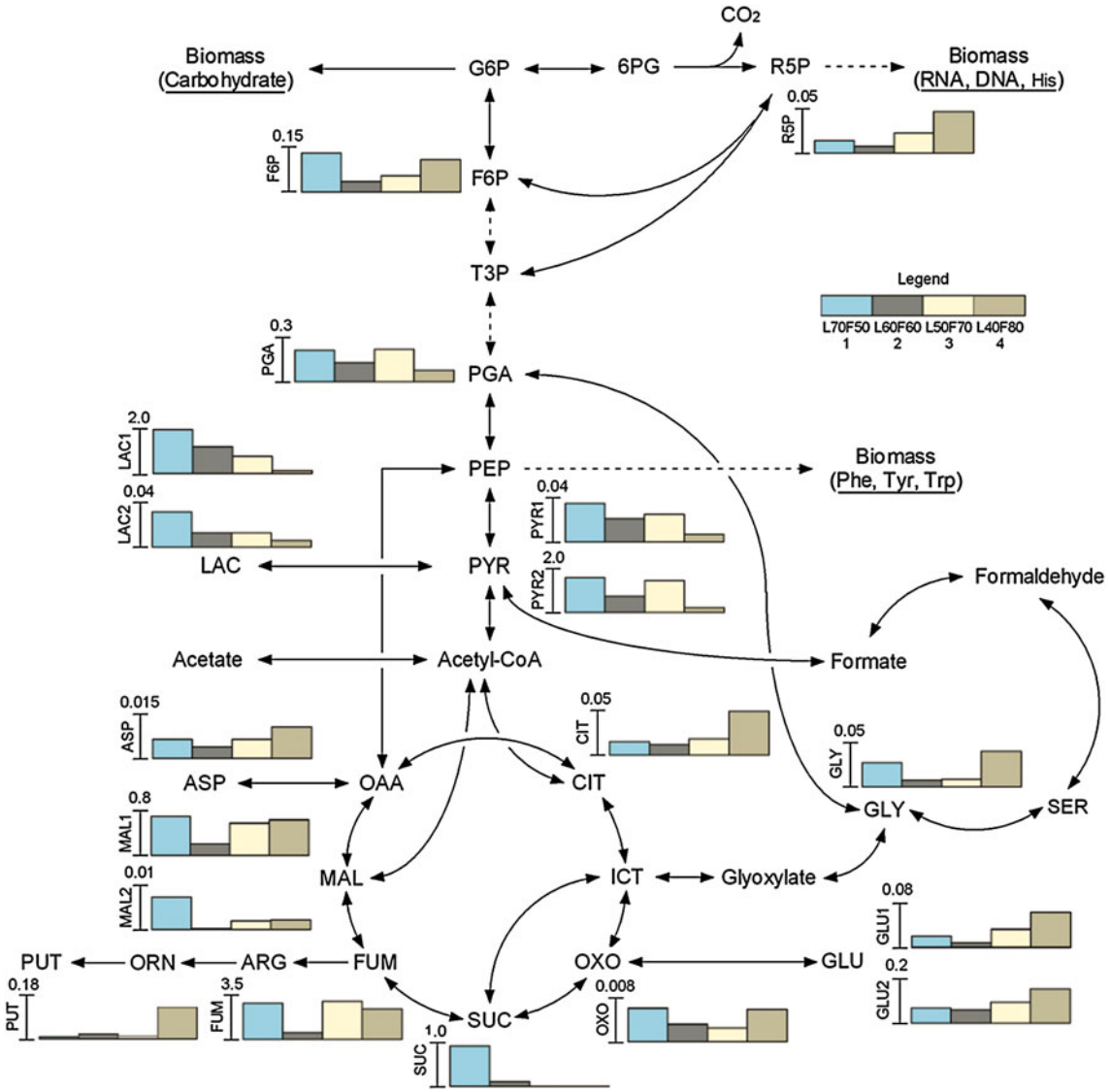

Fig. 4 Intracellular Metabolism Pathway Network of *S. oneidensis* MR-1 grown in minimal medium with four different electron donor and acceptor ratios. *Arrows* represent the directionality of the enzymes and *dotted lines* for pathways where there are multiple intermediates. For the metabolites that are measured the relative abundances of these are shown as inset histograms; the numbers on the ordinate represent the relative abundance to the internal standards run on GC–MS. *Abbreviations*: *ALA* alanine, *ARG* arginine, *ASP* aspartic acid, *CIT* citric acid, *F6P* sugar phosphate, *FUM* fumarate, *G6P* glucose 6-phosphate, *GLC* glucose, *GLU* glutamic acid, *GLY* glycine, *ICT* iso-citrate, *LAC* lactic acid, *LAD* lactic acid, *dimer LEU* leucine, *MAL* malic acid, *ORN* ornithine, *OXO* oxoglutaric acid, *PGA* glycerol-3-phosphate, *PEP* phosphoenolpyruvic acid, *PUT* putrescine, *PYR* pyruvic acid, *R5P* ribose-5-phosphate, *SER* serine, *SPH* sugar phosphate, *SUC* succinic acid, *VAL* valine, *6PG* 6-phosphogluconate. The *error bars* for the metabolites in this pathway are shown in Supplementary information Fig. S3

ornithine (ORN) (neither of which were detected) and finally putrescine in cells grown with high concentration of fumarate as the electron acceptor. This is evidence that excessive fumarate was removed by conversion to putrescine via a branch reaction around the main TCA cycle (Fig. 4).

In addition to the accumulation of the electron acceptor fumarate, other TCA cycle intermediates were detected within the cell. They were present across the spectrum of donor: acceptor ratios, but did tend to accumulate at lower concentrations when the lactate and fumarate were stoichiometrically balanced (60 mM lactate: 60 mM fumarate).

4 Discussion

In this study we have demonstrated that *S. oneidensis* MR-1 can be cultured at steady state under anaerobic conditions in a chemostat and the physiological responses

associated with changes in growth rate and electron donor: acceptor limitation dissected. This has given us considerable insight into the mechanisms of reduction of a model electron acceptor, the azo dye remazol black B, and highlighted optimisation strategies for a broad range of reductive transformations catalysed by this Fe(III)-reducing bacterium (Pearce et al. 2006; Tang et al., 2007c; Wang et al. 2010b). Although manipulation of growth rate in the chemostat through control of the dilution rate did alter biomass yields, it had surprisingly little impact on key physiological parameters including the total cytochrome content of the cells, the production of extracellular flavin redox shuttles or the specific rate of dye reduction in the absence of added extracellular riboflavin. Interestingly, the highest rate of dye reduction with added riboflavin was obtained with cultures grown at the lowest dilution rate, which could correlate with the comparatively low growth rate expected in the organism's usual ecological niche, e.g. the subsurface. Consistent with these results was the lack of significant alterations in the metabolic fingerprints of the cells collected using FT-IR spectroscopy. There was, however, a far more pronounced impact on the physiological parameters that we quantified when the electron donor to acceptor ratio was altered. It is well known that the nature of the electron acceptor can have a dramatic impact on the physiology of *Shewanella* cells, expressed for example as contrasting transcriptome responses (Beliaev et al. 2005) However, the impact of controlling the ratios of electron donor and acceptor has not been studied in detail previously, although it is clearly an important parameter that needs to be optimised for biotechnological applications that utilise the reductive potential of this metabolically flexible facultative anaerobe. Investigations of this kind will also give important insight into the ecophysiology of the organism under environmentally relevant conditions, for example under conditions of electron acceptor limitation when growing on poorly soluble mineral phases in the subsurface, especially after stimulation by electron donor additions.

Maximal dye reduction rates were noted when cells were grown under conditions of electron acceptor (fumarate) limitation (in 100 mM lactate: 20 mM fumarate minimal medium). When cells were grown under conditions of electron donor (lactate) limitation and excess electron acceptor (fumarate), the specific rate of dye reduction was reduced by two orders of magnitude (Table 2). Specific yields of extracellular flavins (FMN) were similar whether grown under conditions of electron donor or acceptor limitation (Table 1), suggesting that this parameter would not control the rate of dye reduction in cultures. Indeed, although flavin additions (as riboflavin) enhanced the dye reduction activities of the electron donor limited cultures somewhat, the specific rates of reduction in these cultures remained significantly lower than those of cultures grown under conditions of electron acceptor limitation.

The physiological parameter that seemed to have the most pronounced impact on dye reduction activity was the overall cytochrome content of the cell. This was reduced by a factor of 10 when the cells were grown under conditions of electron donor limitation (Fig. 2a). This would seem to be consistent with work from our laboratory (Von Canstein and Lloyd, unpublished) and other workers (Russ et al. 2000; Robinson et al. 2001; Rau et al. 2002) which have confirmed the involvement of *c*-type cytochromes including CymA in electron transfer from the cytoplasmic membrane, through the periplasm and potentially to the outer membrane. Interestingly, at intermediate lactate: fumarate ratios (in 60 mM lactate: 60 mM fumarate minimal medium) cytochrome content remained high, although specific dye reduction rates without added riboflavin were reduced when compared to those of cells grown with the lowest electron acceptor concentrations. The addition of riboflavin to the intermediate "60 mM lactate: 60 mM fumarate" grown cells did result in an increase in the specific rate of dye reduction to a rate approaching that noted in the 100 mM lactate: 20 mM fumarate minimal medium (fumarate-limited cultures). This would seem to suggest that there are additional factors other than the total cytochrome yield that control the reductive potential of the cells. This also includes the precise make up of the cytochrome chain, which can potentially include many of the 42 *c*-type cytochromes potentially encoded by the *S. oneidensis* genome. Although outside of the scope of the present investigation this warrants further study. For example, it is important to quantify the abundance of surface localised cytochromes most likely to play a role in extracellular dye reduction in the absence of a redox mediator. It is accepted that microbial reduction of azo dyes is predominantly an extracellular process as these molecules contain sulfonate groups which impede diffusion across cellular membranes (Kudlich et al. 1997). Previous studies have also shown that azo dye reduction by *Shewanella* cells is located in the membrane fraction of the cell while periplasmic and cytoplasmic fractions have no significant activity against these substrates (Hong et al. 2007).

It is well known in other organisms that intracellular metabolism is carefully controlled to achieve a combination of maximal overall growth yield and minimal overall fluxes through the metabolic network (Schuetz et al. 2007). One particular novel aspect of our study was the inclusion of metabolic profiling and we used GC–MS to assess the relationships between metabolites to provide a rich and informative description of the biochemical fingerprints of cellular processes when *S. oneidensis* MR-1 is cultured

under different electron donor and acceptor ratios. Clustering via principal components analysis (Fig. 2) and a Bayesian network (Fig. 3) revealed such relationships, and the latter was used to build a graphical model of the correlations among the metabolites of interest (Correa and Goodacre 2011). The correlations encoded in this graphical model provide accurate information about the underlying interactions among these metabolites and allowed further inference when displayed on a metabolic map of intracellular central metabolism (Fig. 4). Using such approaches, we show that under conditions of electron acceptor limitation, there is evidence of both stored reducing power (as lactate and pyruvate) and high cytochrome content, which can support high rates of electron acceptor (dye) reduction noted earlier. Under conditions of electron acceptor excess there is evidence of metabolites being shunted away from dye and metal-reduction pathways, to non-energy yielding pathways such as the formation of secondary metabolites (e.g. putrescine) and also biomass formation. Thus under conditions of electron acceptor limitation, the central metabolism of *Shewanella* would seem to be streamlined to prevent the dissipation of metabolites, and hence potential reducing power, away from cytochrome-mediated dye and metal reduction pathways. Energy conservation within this highly metabolically flexible organism is clearly very tightly regulated.

Interestingly, although previous studies have suggested that extracellular proteinaceous nanowires may play a role in extracellular electron transfer, especially under conditions of electron acceptor limitation (Gorby et al. 2006), we found no evidence for the presence of this potential mechanism in this chemostat study (Fig. 3). Thus, extracellular nanowires would seem to play no role in the reduction of azo dyes, or other substrates, under the wide range of conditions tested in this study.

5 Concluding remarks

To conclude, these results confirm that it is possible to study and control reductive metabolism of *Shewanella* species using chemostat cultures. We have shown that cultures have maximal activities against a model extracellular electron acceptor when grown under conditions of electron acceptor limitation. These observations give an important insight into the control of *Shewanella* metabolism under conditions of electron acceptor limitation in a range of environments potentially inhabited by *Shewanella* species and other Fe(III)-reducing prokaryotes, for example in the subsurface. These data also suggest optimization strategies to obtain maximal activity for *ex situ* bioprocesses such as the reduction and subsequent degradation of azo dyes (Pearce et al. 2006) and other biotechnological processes catalysed by this important model organism.

Acknowledgments This research was supported by BBSRC grant BBS/B/03718 and a Manchester-CSC PhD scholarship to H Wang. Harald von Canstein and Georgios D. Antoniou are acknowledged for initial discussions on *Shewanella* physiology. E. C. and R. G. would like to thank the Seventh Framework Programme (CommonSense project—SEC-2010.1.3-3 ref: 261809) for financial support. RG and WD thank BBSRC and EPSRC for financial support of the Manchester Centre for Integrative Systems Biology.

References

Alm, E. J., Huang, K. H., Price, M. N., Koche, R. P., Keller, K., Dubchak, I. L., et al. (2005). The microbes online web site for comparative genomics. *Genome Research, 15*, 1015–1022.

Begley, P., Francis-McIntyre, S., Dunn, W. B., Broadhurst, D. I., Halsall, A., Tseng, A., et al. (2009). Development and performance of a gas chromatography time-of-flight mass spectrometry analysis for large-scale nontargeted metabolomic studies of human serum. *Analytical Chemistry, 81*, 7038–7046.

Beliaev, A. S., Klingeman, D. M., Klappenbach, J. A., Wu, L., Romine, M. F., Tiedje, J. M., et al. (2005). Global transcriptome analysis of *Shewanella oneidensis* MR-1 exposed to different terminal electron acceptors. *Journal of Bacteriology, 187*, 7138–7145.

Berry, E. A., & Trumpower, B. L. (1987). Simultaneous determination of hemes *a*, *b*, and *c* from pyridine hemochrome spectra. *Analytical Biochemistry, 161*, 1–15.

Brown, M., Dunn, W. B., Dobson, P., Patel, Y., Winder, C. L., Francis-McIntyre, S., et al. (2009). Mass spectrometry tools and metabolite-specific databases for molecular identification in metabolomics. *Analyst, 134*, 1322–1332.

Brown, M., Dunn, W. B., Ellis, D. I., Goodacre, R., Handl, J., Knowles, J. D., et al. (2005). A metabolome pipeline: from concept to data to knowledge. *Metabolomics, 1*, 39–51.

Clarke, T. A., Edwards, M. J., Gates, A. J., Hall, A., White, G. F., Bradley, J., et al. (2011). Structure of a bacterial cell surface decaheme electron conduit. *Proceedings of the National Academy of Sciences, 108*, 9384–9389.

Coates, J. D., & Achenbach, L. A. (2002). *The Biogeochemistry of Aquifer Systems: Manual of Environmental Microbiology*. Washington, DC: ASM Press.

Cooper, G. F., & Herskovits, E. (1992). A Bayesian method for the induction of probabilistic networks from data. *Machine Learning, 9*, 309–347.

Cornish-Bowden, A., & Luz Cardenas, M. (2000). From genome to cellular phenotype: A role for metabolic flux analysis. *Nature Biotechnology, 18*, 267–268.

Correa, E., & Goodacre, R. (2011). A genetic algorithm-Bayesian network approach for the analysis of metabolomics and spectroscopic data: Application to the rapid identification of *Bacillus* spores and classification of *Bacillus* species. *BMC Bioinformatics, 12*, 33.

Coursolle, D., & Gralnick, J. A. (2010). Modularity of the Mtr respiratory pathway of *Shewanella oneidensis* strain MR-1. *Molecular Microbiology, 77*, 995–1008.

Dunn, W. B., Broadhurst, D. I., Atherton, H. J., Goodacre, R., & Griffin, J. L. (2011a). Systems level studies of mammalian metabolomes: The roles of mass spectrometry and nuclear magnetic resonance spectroscopy. *Chemical Society Reviews, 40*, 387–426.

Dunn, W. B., Broadhurst, D., Begley, P., Zelena, E., Francis-McIntyre, S., Anderson, N., et al. (2011b). Procedures for large-scale metabolic profiling of serum and plasma using gas chromatography and liquid chromatography coupled to mass spectrometry. *Nature Protocols, 6*, 1060–1083.

Goodacre, R., Broadhurst, D., Smilde, A., Kristal, B., Baker, J., Beger, R., et al. (2007). Proposed minimum reporting standards for data analysis in metabolomics. *Metabolomics, 3*, 231–241.

Goodacre, R., Vaidyanathan, S., Dunn, W. B., Harrigan, G. G., & Kell, D. B. (2004). Metabolomics by numbers: Acquiring and understanding global metabolite data. *Trends in Biotechnology, 22*, 245–252.

Gorby, Y. A., Yanina, S., McLean, J. S., Rosso, K. M., Moyles, D., Dohnalkova, A., et al. (2006). Electrically conductive bacterial nanowires produced by *Shewanella oneidensis* strain MR-1 and other microorganisms. *Proceedings of the National Academy of Sciences of the United States of America, 103*, 11358–11363.

Heidelberg, J., Paulsen, I. T., Nelson, K. E., Gaidos, E. J., Nelson, W. C., Read, T. D., et al. (2002). Genome sequence of the dissimilatory metal ion-reducing bacterium *Shewanella oneidensis*. *Nature Biotechnology, 20*, 1118–1123.

Hernandez, M. E., & Newman, D. K. (2001). Extracellular electron transfer. *Cellular and Molecular Life Sciences, 58*, 1562–1571.

Hong, Y. G., Chen, X. J., Guo, J., Xu, Z. C., Xu, M. Y., & Sun, G. P. (2007). Effects of electron donors and acceptors on anaerobic reduction of azo dyes by *Shewanella decolorationis* S12. *Applied Microbiology and Biotechnology, 74*, 230–238.

Johnson, R. A., & Wichern, D. W. (2007). *Applied multivariate statistical analysis* (6th ed.). Pearson: Prentice Hall. ISBN: 0-13-187715-1.

Kopka, J., Schauer, N., Krueger, S., Birkemeyer, C., Usadel, B. R., Bergmaller, E., et al. (2005). GMD@CSB.DB: The Golm Metabolome Database. *Bioinformatics, 21*, 1635–1638.

Kudlich, M., Keck, A., Klein, J., & Stolz, A. (1997). Localization of the Enzyme System Involved in Anaerobic Reduction of Azo Dyes by Sphingomonas sp. Strain BN6 and Effect of Artificial Redox Mediators on the Rate of Azo Dye Reduction. *Applied and Environment Microbiology, 63*, 3691–3694.

Lovley, D. R., Coates, J. D., Blunt-Harris, E. L., Philips, E. J. P., & Woodward, J. C. (1996). Humic substances as electron for microbial respiration. *Nature, 382*, 445–448.

MacKenzie, D. A., Defernez, M., Dunn, W. B., Brown, M., Fuller, L. J., de Herrera, S. R. M. S., et al. (2008). Relatedness of medically important strains of *Saccharomyces cerevisiae* as revealed by phylogenetics and metabolomics. *Yeast, 25*, 501–512.

Marsili, E., Baron, D. B., Shikhare, I. D., Coursolle, D., Gralnick, J. A., & Bond, D. R. (2008). *Shewanella* secretes flavins that mediate extracellular electron transfer. *Proceedings of the National Academy of Sciences, 105*, 3968–3973.

Martens, H., & Stark, E. (1991). Extended multiplicative signal correction and spectral interference subtraction-new preprocessing methods for near infrared spectroscopy. *Journal of Pharmaceutical and Biomedical Analysis, 9*, 625–635.

Myers, C. R., & Myers, J. M. (1992). Localization of cytochromes to the outer membrane of anaerobically grown *Shewanella putrefaciens* MR-1. *Journal of Bacteriology, 174*, 3429–3438.

Myers, C. R., & Myers, J. M. (1993). Ferric reductase is associated with the membranes of anaerobically grown *Shewanella putrefaciens* MR-1. *FEMS Microbiology Letters, 108*, 15–21.

Myers, C. R., & Myers, J. M. (1997a). Isolation and characterization of a transposon mutant of *Shewanella putrefaciens* MR-1 deficient in fumarate reductase. *Letters in Applied Microbiology, 25*, 162–168.

Myers, C. R., & Myers, J. M. (1997b). Cloning and sequence of *cymA*, a gene encoding a tetraheme cytochrome *c* required for reduction of iron(III), fumarate and nitrate by *Shewanella putrefaciens* MR-1. *Journal of Bacteriology, 179*, 1143–1152.

Myers, J. M., & Myers, C. R. (2000). Role of tetraheme cytochrome CymA in anaerobic electron transport in cells of *Shewanella putrefaciens* MR-1 with normal levels of menaquinone. *Journal of Bacteriology, 182*, 67–75.

Myers, C. R., & Myers, J. M. (2004). *Shewanella oneidensis* MR-1 restores menaquinone synthesis to a menaquinone-negative mutant. *Applied and Environmental Microbiology, 70*, 5415–5425.

Myers, C. R., & Nealson, K. H. (1990). Respiration-linked proton translocation coupled to anaerobic reduction of manganese(IV) and iron(III) in *Shewanella putrefaciens* MR-1. *Journal of Bacteriology, 172*, 6232–6238.

Newman, D. K., & Kolter, R. (2000). A role for excreted quinones in extracellular electron transfer. *Nature, 405*, 94–97.

O'Hagan, S., Dunn, W. B., Brown, M., Knowles, J. D., & Kell, D. B. (2004). Closed-loop, multiobjective optimization of analytical instrumentation:gas chromatography/time-of-flight mass spectrometry of the metabolomes of human serum and of yeast fermentations. *Analytical Chemistry, 77*, 290–303.

Pearce, C. I., Christie, R., Boothman, C., von Canstein, H., Guthrie, J. T., & Lloyd, J. R. (2006). Reactive azo dye reduction by *Shewanella* strain J18 143. *Biotechnology and Bioengineering, 95*, 692–703.

Pearl, J. (1988). *Probabilistic reasoning in intelligent systems: Networks of plausible inference*. San Mateo, CA: Morgan Kaufmann.

Pearl, J. (2000). *Causality: Models, reasoning and inference*. Cambridge, UK: Cambridge University Press.

Rau, J., Knackmuss, H.-J., & Stolz, A. (2002). Effects of different quinoid redox mediators on the anaerobic reduction of azo dyes by bacteria. *Environmental Science and Technology, 36*, 1497–1504.

Reguera, G., McCarthy, K. D., Mehta, T., Nicoll, J. S., Tuominen, M. T., & Lovley, D. R. (2005). Extracellular electron transfer via microbial nanowires. *Nature, 435*, 1098–1101.

Robinson, T., McMullan, G., Marchant, R., & Nigam, P. (2001). Remediation of dyes in textile effluent: A critical review on current treatment technologies with a proposed alternative. *Bioresource Technology, 77*, 247–255.

Russ, R., Rau, J., & Stolz, A. (2000). The function of cytoplasmic flavin reductases in the reduction of azo dyes by bacteria. *Applied and Environmental Microbiology, 66*, 1429–1434.

Schuetz, R., Kuepfer, L., & Sauer, U. (2007). Systematic evaluation of objective functions for predicting intracellular fluxes in *Escherichia coli*. *Molecular Systems Biology, 3*, 119.

Serres, M. H., & Riley, M. (2006). Genomic analysis of carbon source metabolism of *Shewanella oneidensis* MR-1: Predictions versus experiments. *Journal of Bacteriology, 188*, 4601–4609.

Sumner, L., Amberg, A., Barrett, D., Beale, M., Beger, R., Daykin, C., et al. (2007). Proposed minimum reporting standards for chemical analysis. *Metabolomics, 3*, 211–221.

Tang, Y. J., Chakraborty, R., Martin, H. G., Chu, J., Hazen, T. C., & Keasling, J. D. (2007a). Flux analysis of central metabolic pathways in geobacter metallireducens during reduction of soluble Fe(III)-nitrilotriacetic acid. *Applied and Environmental Microbiology, 73*, 3859–3864.

Tang, Y. J., Hwang, J. S., Wemmer, D. E., & Keasling, J. D. (2007b). *Shewanella oneidensis* MR-1 fluxome under various oxygen conditions. *Applied and Environmental Microbiology, 73*, 718–729.

Tang, Y. J., Meadows, A. L., Kirby, J., & Keasling, J. D. (2007c). Anaerobic central metabolic pathways in *Shewanella oneidensis* MR-1 reinterpreted in the light of isotopic metabolite labeling. *Journal of Bacteriology, 189*, 894–901.

Taylor, P., Pealing, S. L., Reid, G. A., Chapman, S. K., & Walkinshaw, M. D. (1999). Structural and mechanistic mapping

of a unique fumarate reductase. *Nature Structural Biology, 6*, 1108–1112.

von Canstein, H., Ogawa, J., Shimizu, S., & Lloyd, J. R. (2008). Secretion of flavins by *Shewanella* species and their role in extracellular electron transfer. *Applied and Environmental Microbiology, 74*, 615–623.

Wang, H., Hollywood, K., Jarvis, R. M., Lloyd, J. R., & Goodacre, R. (2010a). Phenotypic characterization of *Shewanella oneidensis* MR-1 under aerobic and anaerobic growth conditions by using Fourier Transform Infrared Spectroscopy and High-Performance Liquid Chromatography analyses. *Applied and Environmental Microbiology, 76*, 6266–6276.

Wang, H., Law, N., Pearson, G., van Dongen, B. E., Jarvis, R. M., Goodacre, R., et al. (2010b). Impact of silver(I) on the metabolism of *Shewanella oneidensis*. *Journal of Bacteriology, 192*, 1143–1150.

Winder, C. L., Dunn, W. B., & Goodacre, R. (2011). TARDIS-based microbial metabolomics: Time and relative differences in systems. *Trends in Microbiology, 19*, 315–322.

Winder, C. L., Dunn, W. B., Schuler, S., Broadhurst, D., Jarvis, R., Stephens, G. M., et al. (2008). Global metabolic profiling of *Escherichia coli* cultures: An evaluation of methods for quenching and extraction of intracellular metabolites. *Analytical Chemistry, 80*, 2939–2948.